https://doi.org/10.5194/amt-2023-137
Preprint. Discussion started: 13 July 2023

Atmospheric Measurement Techniques Discussions

Closing the gap in the tropics: the added value of radio-occultation data for wind field monitoring across the equator

Julia Danzer[1], Magdalena Pieler[1], and Gottfried Kirchengast[1,2]

[1]Wegener Center for Climate and Global Change, University of Graz, Graz, 8010, Austria
[2]Institute of Physics, University of Graz, Graz, 8010, Austria

Correspondence: Julia Danzer (julia.danzer@uni-graz.at)

Abstract. Globally available and highly vertical resolved wind fields are crucial for the analysis of atmospheric dynamics for the benefit of climate studies. Most observation techniques have problems to fulfill both requirements. Especially in the tropics and in the southern hemisphere more wind data availability is required. In this study we investigate the potential of radio occultation (RO) data for climate-oriented wind field monitoring in the tropics, with a specific focus on the equatorial area between $\pm 5°$ latitude. In this region, the geostrophic balance breaks down, due to the Coriolis force term approaching zero. One further aim is to understand how the individual wind components of the geostrophic balance and equatorial balance approximations bridge across the equator and where each component breaks down. We analyze the equatorial balance equation within this latitude band. In a wider range over the tropics, we derive the RO wind fields also using the geostrophic approximation and we compared the RO winds with ERA5 data. From analyzing first the zonal and meridional wind component, we find that the meridional wind component is more volatile in its derivation, however the total wind speed benefits from a computation of both wind components. Investigating next the bias between the RO and ERA5 computed winds, we find that the systematic data bias is smaller than the bias resulting from the approximation itself. As a final aspect we inspected the monthly-mean RO wind data over the full example year 2009. The bias in the upper troposphere and lower stratosphere is mainly smaller than $\pm 2\,\mathrm{ms}^{-1}$, which is in line with the wind field requirements of the World Meteorological Organization. This is encouraging for the use of RO wind fields in climate monitoring over the entire globe including the equatorial region.

1 Introduction

Globally available upper air wind profiling information is crucial for the analysis of atmospheric dynamics for the benefit of climate studies, as well as climate models and numerical weather prediction. To determine a wind flow in its full state, wind sensitive measurements need to ensure a high, 3-dimensional resolution, global coverage, and frequent observations from the troposphere to the stratosphere (English et al., 2013; Bauer et al., 2015; Eyre et al., 2020). However, wind measurements in the free atmosphere, depending on the observing system, lack very often one or these requirements.

Stoffelen et al. (2005, 2020) emphasize the need for horizontal resolutions smaller than 500 km to 10 km, to follow an atmospheric process in detail from initial small-scale amplitudes to evolving dynamical mesoscale structures. The World Meteorological Organization (WMO) and the Observing Systems Capability Analysis and Review tool (OSCAR) require a vertical

https://doi.org/10.5194/amt-2023-137
Preprint. Discussion started: 13 July 2023


Atmospheric Measurement Techniques Discussions

wind information of about $1\,\mathrm{km}$ in the troposphere and $2\,\mathrm{km}$ in the stratosphere, for weather and climate applications, with a wind accuracy of $2\,\mathrm{m\,s^{-1}}$ (see WMO-OSCAR, 2023).

Furthermore, well-resolved wind data need to be available over the oceans, tropics, and Southern Hemisphere, where often a measurement gap is present. For example, land surface stations, ships, buoys, and wind scatterometers from satellites provide valuable surface data, but lack vertical profiling information. Aircrafts and atmospheric motion vectors (AMVs) from geostationary or polar satellites provide a high temporal and horizontal sampling at several heights, but lack global representation. Wind profiler, radio sondes, and pilot balloons, have a high vertical sampling, however having information primarily at single locations over continents and the Northern Hemisphere. On the other hand, the Atmospheric Dynamics Mission (ADM-Aeolus) has the potential of 3D wind profiling with a frequent and high resolution coverage, filling measurement gaps over the oceans, poles, tropics, and the Southern Hemisphere up to an altitude of about 20 km. However, it depends on clear air molecular scattering (no measurements within clouds), which can be particularly tricky at tropical latitudes, due to the high-altitude cloud systems (see also, Stoffelen et al., 2005, 2020; Kanitz et al., 2019).

In this respect, a valuable complementary data source comes from exploiting a different satellite based observation technique, the Global Navigation Satellite System (GNSS) radio occultation (RO) method. RO provides vertical profiles of geophysical variables such as bending angle, refractivity, pressure, density, and temperature. A basic introduction to the RO method can be found in, e.g., Kursinski et al. (1997); Hajj et al. (2002). The applications range across climate monitoring and climate analysis, numerical weather prediction, as well as space weather applications (e.g., Healy, 2007; Cucurull, 2010; Foelsche et al., 2009; Anthes, 2011; Steiner et al., 2011).

There are several key advantages of RO data, which could make them a beneficial observation-based data set for indirect wind field monitoring. First of all, it provides a multi-satellite, long-term stable, global data set record, with no need for intercalibration between the missions (Wickert et al., 2001; Anthes et al., 2008; Foelsche et al., 2011; Angerer et al., 2017; Steiner et al., 2020). In addition, the radio occultation method provides all-weather capability. This is a specific advantage in the tropics with large high-altitude cloud systems, that can limit other observation systems, such as optical sounders. Furthermore, RO data is a high vertical resolution data set, with a resolution of about $100\,\mathrm{m}$ to $200\,\mathrm{m}$ in the troposphere, to about $500\,\mathrm{m}$ in the lower stratosphere at low to mid-latitudes, and near $1.5\,\mathrm{km}$ from the middle stratosphere towards high latitudes (Schwarz et al., 2017, 2018; Zeng et al., 2019). RO data cover well the complete stratosphere, with a core region of high quality between about $5\,\mathrm{km}$ to $35\,\mathrm{km}$ altitude (Zeng et al., 2019; Steiner et al., 2020). Hence it can give additional wind profiling information in high altitude regions, where other observation based data sets might only cover the troposphere and the lower stratosphere (e.g., radiosondes, Ladstädter et al. (2015); Bodeker et al. (2016)).

Traditionally, most RO climate studies concentrate on using the high-quality vertical temperature information (e.g., Li et al., 2023; Ladstädter et al., 2023). With respect to numerical weather prediction, the RO bending angle and refractivity profiles (on altitude levels) are assimilated in forecasting and reanalysis systems (e.g., Kuo et al., 2000; Cardinali and Healy, 2014; Hersbach et al., 2020). One aspect, emphasized in Scherllin-Pirscher et al. (2017), is hereby of particular importance. RO measurements have the power of vertical geolocation, meaning they can give accurate information on the absolute position of a measured air parcel. Hence, RO provides virtually independent information on altitude and pressure fields, enabling

https://doi.org/10.5194/amt-2023-137
Preprint. Discussion started: 13 July 2023

Atmospheric Measurement Techniques Discussions

also to study a very accurate representation of the mass field driven wind field circulation. So far, only a few studies have analyzed the option of calculating wind fields from RO geopotential fields, on isobaric levels. Scherllin-Pirscher et al. (2014) and Verkhoglyadova et al. (2014) have tested the geostrophic wind approximation, excluding the tropics completely between $15°$ and $10°$, North and South, respectively. Healy et al. (2020), on the other hand, tested the zonal equatorial balance equation around the equator, studying a 5°-zonal band for RO data.

In a previous study, Nimac et al. (2023) started to analyze the geostrophic approximation on a monthly 2.5° x 2.5° latitude x longitude grid for ERA5-reanalysis and RO data. It was possible to reproduce the original winds rather well, and within the target of $\pm 2\,\mathrm{ms}^{-1}$. The exception with somewhat higher deviations were strong wind speeds, such as in regions of the jet stream, and over large mountain areas (e.g., Himalayan or Anthes region), where the ageostrophic contributions grow in importance. In general, the wind speed estimates performed well towards the tropics up to even $\pm 5°$ around the equator band, going further towards the equator than other prior RO studies. Within the equator band the Coriolis force converges towards zero and the singularity starts to dominate. Interesting was also to see, when studying the temporal stability between RO and ERA5 geostrophic winds from 2007 and 2020, the differences became noticeably smaller in the year 2016, when ERA5 had observing system changes. This emphasizes the temporal stability of RO data, and since differences became smaller, this also points to the high-quality of RO data.

In this study we aim to close the gap in RO wind field computation across the equator. For this purpose we investigate the zonal and meridional wind components, as well as total wind speed, based on the equatorial balance equation (Chandra et al., 1990; Scaife et al., 2000; Holton, 2004). The method and used data sets are introduced in Section 2 and Section 3. In a first step, we assess the quality of the approximation, using monthly ERA5 reanalysis data (Hersbach et al., 2020) on a 2.5° x 2.5° latitude x longitude grid as a reference. Here we compare the original ERA5 wind components and wind speeds to the ones computed from the equatorial balance approximation (Section 4.1). In a second step, we derive the zonal and meridional wind components, as well as total wind speed, for monthly RO climatologies, analyzing the quality and added value of RO wind field products over the equatorial band (Section 4.2). Finally, in Section 4.3, we test how the equatorial-balanced wind speeds bridge the geostrophic wind speeds across the equator, closing the gap in the tropics with RO wind data. Summary and Conclusions are then given in Section 5.

2 Method for wind field derivation

In general a wind flow in the free atmosphere can be approximated by geostrophic balance, which equals an exact balance between Coriolis force and pressure gradient force. Friction can be ignored in the free atmosphere, while ageostrophic contributions become generally of higher relevance in the winter hemisphere, and also above large mountain areas (see e.g., Scaife et al., 2000; Nimac et al., 2023). When winds are studied at the equator, the geostrophic balance breaks down, due to the Coriolis force approaching zero, inducing a singularity in the geostrophic approximation. A solution for the wind equation in the tropics, assuming a steady friction-less flow, is the equatorial balance equation. In this study we calculate wind speeds, using the geostrophic balance and equatorial balance approximations, with the main focus on the latter one. The derivation of

https://doi.org/10.5194/amt-2023-137
Preprint. Discussion started: 13 July 2023

Atmospheric Measurement Techniques Discussions

RO wind fields, based on the geostrophic approximation, has already been thoroughly validated in a prior study (Nimac et al., 2023). In our analysis we follow the accruracy requirements specified by the World Meteorological Organization (WMO), see WMO-OSCAR, 2023. A target requirement for wind speed biases are hereby values smaller than $\pm 2\,\mathrm{m\,s^{-1}}$, with a maximal bias threshold of $\pm 5\,\mathrm{m\,s^{-1}}$.

The equatorial balance equation: to derive wind fields over the equator, we follow the formulation of Chandra et al. (1990); Scaife et al. (2000). The equatorial wind data are derived from geopotential Φ, given on isobaric levels, resulting in the following formulation for the zonal and meridional wind components, u_{eb} and v_{eb}, respectively, over the equator:

$$u_{eb} \simeq -\frac{1}{\beta}\frac{\partial \Phi^2}{\partial y^2}\,, \tag{1}$$

$$v_{eb} \simeq \frac{1}{\beta}\cos\varphi\frac{\partial \Phi^2}{\partial y \partial x}\,, \tag{2}$$

where β equals $2\Omega/R_\mathrm{E}$, with Ω being the Earth's angular rotation rate (7.2921×10^{-5} rad/s), and R_E is the Earth's mean radius ($6371\,\mathrm{km}$). The derivative of the geopotential Φ is taken in northward, y, and eastward, x, direction. In our analysis, the derivative has been implemented with the forward finite-difference method.

The geostrophic balance equation: to derive wind fields outside the equator region, the geostrophic balance equation is used (e.g., Scherllin-Pirscher et al., 2014). The wind components are still derived from geopotential Φ, given on isobaric levels, resulting in the following formulation of the geostrophic zonal and meridional wind components, u_g and v_g:

$$u_g \simeq -\frac{1}{f(\varphi)R_\mathrm{E}}\frac{\partial \Phi}{\partial \varphi}\,, \tag{3}$$

$$v_g \simeq \frac{1}{f(\varphi)R_\mathrm{E}\cos\varphi}\frac{\partial \Phi}{\partial \lambda}\,, \tag{4}$$

with $f(\varphi) = 2\Omega\sin\varphi$ being the Coriolis parameter, and φ and λ being the latitude and longitude in degrees, respectively, also implementing these derivatives by the forward finite-difference method.

Wind speed: for both methods we calculated the wind speed as $V = \sqrt{u^2 + v^2}$, where the subscripts in our figures (Sect. 4 and Sect. 4.3) will indicate, whether the wind speed was derived from the equatorial balance (eb) or geostrophic (g) wind field approximation. Furthermore, the original wind speeds from the ERA5 reanalysis data have the subscript (o), indicating the original ERA5 wind data.

Validation: we derived the equatorial winds and the geostrophic winds for the complete globe. However, from our prior analysis we know, that between $\pm 5^\circ$ latitude, the geostrophic approximation breaks down, since it is not the correct physical approximation for the wind retrieval (Nimac et al., 2023). In this region the equatorial balanced winds take over. Hence, we indicate this latitudinal area in all our result figures with a light grey shaded area. Within this area, the validation of the equatorial balance equation is conducted, aiming to bridge the equatorial gap, when deriving RO wind fields. The bias directly obtained from the equatorial balance equation is studied as the difference between ERA5 balanced (eb) and original (o) wind

https://doi.org/10.5194/amt-2023-137
Preprint. Discussion started: 13 July 2023

Atmospheric Measurement Techniques Discussions

speeds, while the systematic difference is studied as the difference between RO and ERA5 balanced winds, as summarized in Table 1:

Bias	**Definition**	**Lat Range**	**Lon Range**
Equatorial-balance bias	$\mathrm{ERA5}_{eb} - \mathrm{ERA5}_{o}$	focus area $\pm 5^\circ$ N/S	all
Systematic data bias	$\mathrm{RO}_{eb,g} - \mathrm{ERA5}_{eb,g}$	focus area $\pm 5^\circ$ N/S (eb); complete globe (g)	all

Table 1. Definition of the equatorial-balance bias and systematic data bias, as well as analyzed latitudinal and longitudinal ranges.

The biases are validated for zonal (u), meridional wind (v), as well as wind speed (V). As mentioned above, the target threshold for data quality is $\pm 2\,\mathrm{m\,s^{-1}}$, with a maximal bias of $\pm 5\,\mathrm{m\,s^{-1}}$, in line with WMO requirements WMO-OSCAR, 2023. The thresholds are marked with dashed lines in the result figures.

3 Data sets

Monthly ERA5 reanalysis data (Hersbach et al., 2020) and monthly averaged RO OPSv5.6 data (Angerer et al., 2017; Steiner et al., 2020) from the year 2009 were used. This year was chosen for its high number of RO observations, representing a good approximation for later years, when the COSMIC-2 mission started (June 2019), which has an especially high number of observations in the tropics and the mid-latitudes. To limit the length of the paper, January was chosen as a representative month for the figure analysis. All other months were studied as well, and are partially shown as part of the results in respective time series plots.

3.1 ERA5 reanalysis data

The ERA5 reanalysis data combines global 3D wind information and geopotential height, it is therefore the ideal data set to test the validity of the equatorial balance equation. It is available for a long time period and readily accessible via download from the Copernicus Climate Data Store (CCDS) (ECMWF-ERA5monthly). The data are available on 37 levels from $1000\,\mathrm{hPa}$ to $1\,\mathrm{hPa}$, on a 0.25°x0.25° grid. Different grid resolutions were investigated for wind derivation, to find the sensible spatial grid, for the equatorial balance approximation. Fig. 1 shows the result for the zonal equatorial balanced wind, u_{eb}, where a) shows the result for the zonal wind component, tested for resolutions from 0.5° up to 5°, and b) shows the difference to the original ERA5 zonal wind component.

The analysis in Fig. 1 illustrates that a grid spacing of 0.5° and 1° is counter productive, as the u component shows large fluctuations. A grid of 2.5° or 3° results in similar values. For a 5° spacing, the loss in resolution is noticeable.

As a result, we chose a 2.5°x2.5° climatology for all further ERA5 wind investigations. The data sets with lower resolutions were derived from the original 0.25°x0.25° grid, via cosine-weighted binning. The wind component data from the reanalysis is labeled u_o, v_o, and V_o, corresponding to the eastward-, northward wind component, and the wind speed. A line above the variable indicates a zonal average, e.g. $\overline{u}_o$. The wind components derived from the geopotenial via the equatorial balance equation are referred to as u_{eb}, v_{eb}, and V_{eb}, or with a subscript g, when we used the geostrophic approximation.

https://doi.org/10.5194/amt-2023-137
Preprint. Discussion started: 13 July 2023

Atmospheric Measurement Techniques Discussions

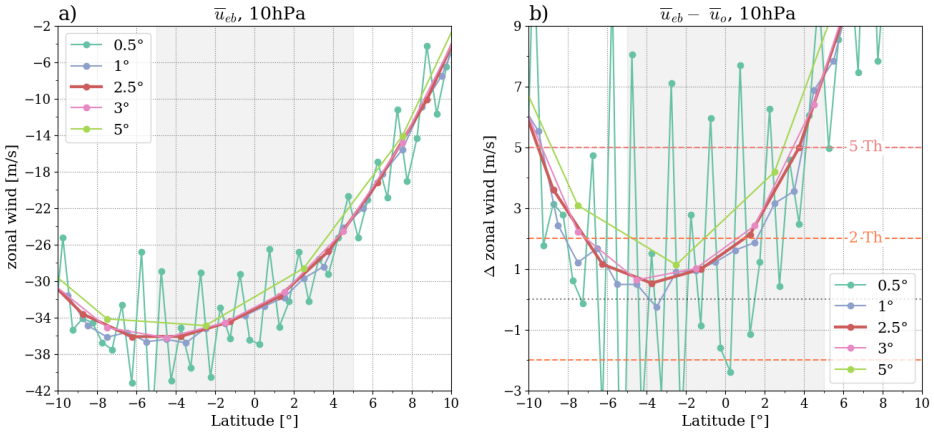

Figure 1. Influence of different spatial resolutions on the zonal-mean wind component. Panel a) shows the wind component, u_{eb}, panel b) the difference of the calculated wind to the ERA5 wind field zonal wind component u_o.

3.2 Radio occultation data

We use monthly RO climatologies data from multi-satellite missions in the year 2009. The RO phase data were derived at UCAR/CDAAC (University Corporation for Atmospheric Research/COSMIC Data Analysis and Archive Center), while the further processing to geopotential height, $Z(p)$, calculated on isobaric surfaces p, was performed using the WEGC Occultation Processing System OPSv5.6 (Angerer et al., 2017; Steiner et al., 2020). The conversion to geopotential $\Phi(p)$ is defined as $\Phi(p) = Z(p) \cdot g_0$, where $g_0 = \pm 9.806\,65\,\mathrm{m/s^2}$, being the global standard gravity at mean sea level. In the year 2009, data is available from the following missions: Satélite de Aplicaciones Científicas (SAC-C) (e.g., Hajj et al., 2004), Gravity Recovery And Climate Experiment (GRACE-A) (e.g., Beyerle et al., 2005), Formosa Satellite Mission 3/Constellation Observing System for Meteorology, Ionosphere, and Climate (Formosat-3/COSMIC) (e.g., Anthes et al., 2008), and from the Meteorological Operational Satellite (MetOp-A) (e.g., Luntama et al., 2008). The year 2009 was chosen as a representative data set to analyze the wind dynamics within a full year, having at the same time the advantage of a rather high occultation statistics, due to the fully available six-satellite constellation of the Formosat-3/COSMIC mission (Angerer et al., 2017).

The monthly climatologies were produced on a 2.5° x 2.5° grid, using a Gaussian latitude-longitude weighting, within a radius of $600\,\mathrm{km}$. The geopotential climatologies $\Phi(p)$ are available from $1000\,\mathrm{hPa}$ to $5\,\mathrm{hPa}$, on 147 levels. The geopotential was further binned to a 5° x 5° grid, using a cosine weighted binning. From this larger bins, the equatorial balanced winds were calculated, applying afterwards a further longitudinal Gaussian window smoothing. The larger binning was performed to avoid small fluctuations in the wind data, which required larger climatologies. Regarding geostrophic winds, the 2.5° x 2.5° grid could be maintained. The most prominent difference in the computation between equatorial and geostrophic winds is that the former requires a double derivative, while the latter requires a single derivative. Hence, small fluctuations in the data are enhanced for the equatorial balance equation, which makes the derivation of winds a bigger challenge. However, we emphasize at this point,

https://doi.org/10.5194/amt-2023-137
Preprint. Discussion started: 13 July 2023

Atmospheric Measurement Techniques Discussions

that due to the COSMIC-2 mission (start in June 2019), which provides a higher sampling in the tropics, the potential of finer resolutions is given (Schreiner et al., 2020; Ho et al., 2020).

For the comparison between calculated ERA5 and RO wind, an interpolated ERA5 reanalysis data set with 364 levels from $1000\,\mathrm{hPa}$ to $10\,\mathrm{hPa}$ was used. Since RO data were binned to a $5°$x$5°$ grid (see Sect. 3.2, to have a sufficient number of observations per grid cell), the ERA5 data set was also transferred to a $5°$x$5°$ grid, using cosine weighted binning. For this specific data set the prefix ERA is used.

4 Results and discussion

To validate the equatorial balance equation, the zonal and meridional wind components, and wind speed were calculated according to the equations introduced in Sect. 2. We analyze the bias from the equatorial balance equation in Sect. 4.1. The systematic bias between the observation-based RO data set and the reanalysis data set, is investigated in Sect. 4.2. Hereby, the potential of RO wind products over the equatorial region is tested. The results on closing the gap across the equator are discussed in Sect. 4.3.

4.1 ERA5 wind validation

To test the quality of the equatorial balance equation, both wind components individually, and the accumulated wind speed are compared to the wind field in ERA5. Fig. 2 shows the original wind and the calculated wind component/wind speed with the equatorial balance equation, as well as the respective difference for January, 2009. For the zonally averaged zonal wind component $\overline{u}_{eb}$, and wind speed $\overline{V}_{eb}$, spatial features of the wind field are well reproduced by the equatorial balance equation, compare Fig. 2 a) and b), as well as g) and h). Fig. 2 c) shows the difference between $\overline{u}_{eb}$ and $\overline{u}_o$. For all levels there is a range in which the difference is below the target threshold of $\pm 2\,\mathrm{m\,s^{-1}}$. Towards lower pressures the approximation becomes less accurate. Fig. 2 d), e) and f) show the same comparisons for the v component. Because the magnitude and direction of meridional wind changes with respect to longitude, the plots show an average around the prime meridian ($-10°$ to $10°$ longitude). The meridional wind bias is below $\pm 2\,\mathrm{m\,s^{-1}}$ everywhere, except around $200\,\mathrm{hPa}$ and close to the surface, where the Hadley cell is situated and friction is not neglectable. Nevertheless, it should be noted that absolute meridional wind speeds, outside of these regions, are small, therefore an absolute threshold might be satisfied, even though there are large relative deviations. In general, the meridional component is not reproduced as well as the zonal wind. This could be due to the fact that the v component contains a derivation with respect to latitude as well as longitude which is computationally not as robust as the second derivative with respect to latitude. One can show that despite the shortcomings of the meridional equatorial approximation, the wind speed is better reproduced when using $V_{eb} = \sqrt{u_{eb}^2 + v_{eb}^2}$ than using $V_{eb} \approx |u_{eb}|$.

In a next step, we investigate the latitudinal scope of the equatorial approximation and the magnitude of the approximation bias. The mean zonal wind, meridional wind and wind speed bias in a zonal latitude band is plotted, see Fig. 3. Comparing Fig. 2 and Fig. 3 shows for a latitude band compared to individual $-2.5°$x$2.5°$ grid cells, that the accuracy of the approximation increases. The wind speed bias in the free atmosphere does not exceed the maximum bias threshold of $\pm 5\,\mathrm{m\,s^{-1}}$ for all bands

https://doi.org/10.5194/amt-2023-137
Preprint. Discussion started: 13 July 2023

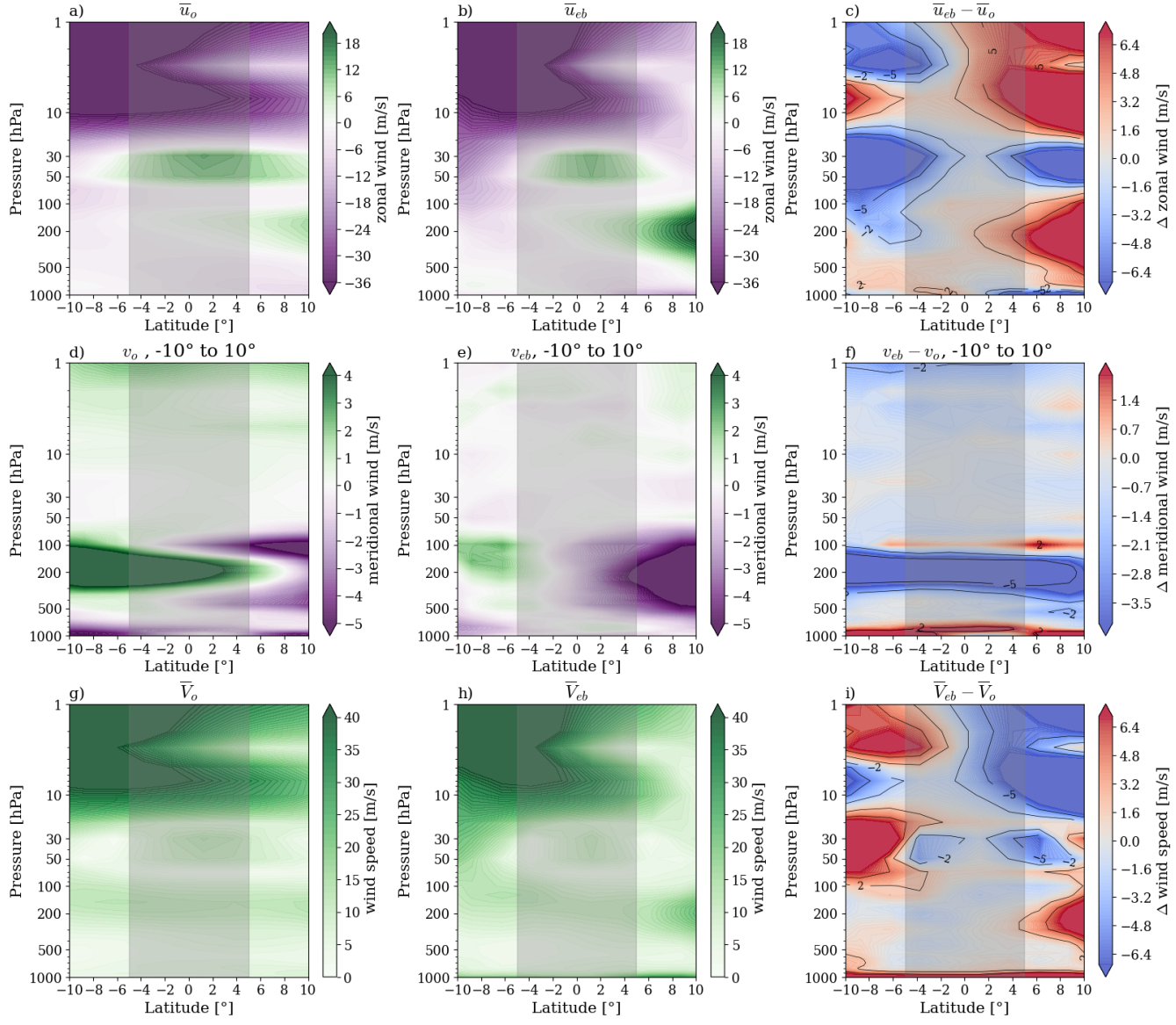

Figure 2. Panels a), d) and g) show the u, v and V component of the original ERA5 data. Panels b), e) and h) show the wind components calculated with the equatorial balance approximation. The bottom row illustrates the difference between the calculated values and the original wind data from ERA5. Note that u and V are plotted as a zonal average, while the v component is shown as the mean of the longitude band $-10°$ to $10°$.

within $-7.5°$ - $7.5°$ latitude. Thus, the equatorial approximation can be used to approximate average equatorial wind speeds in the equatorial region in a latitudinal range of $-7.5°$ to $7.5°$. For $\overline{u}_{eb}$ the increase of the bias with a broadening of the latitudinal

https://doi.org/10.5194/amt-2023-137
Preprint. Discussion started: 13 July 2023

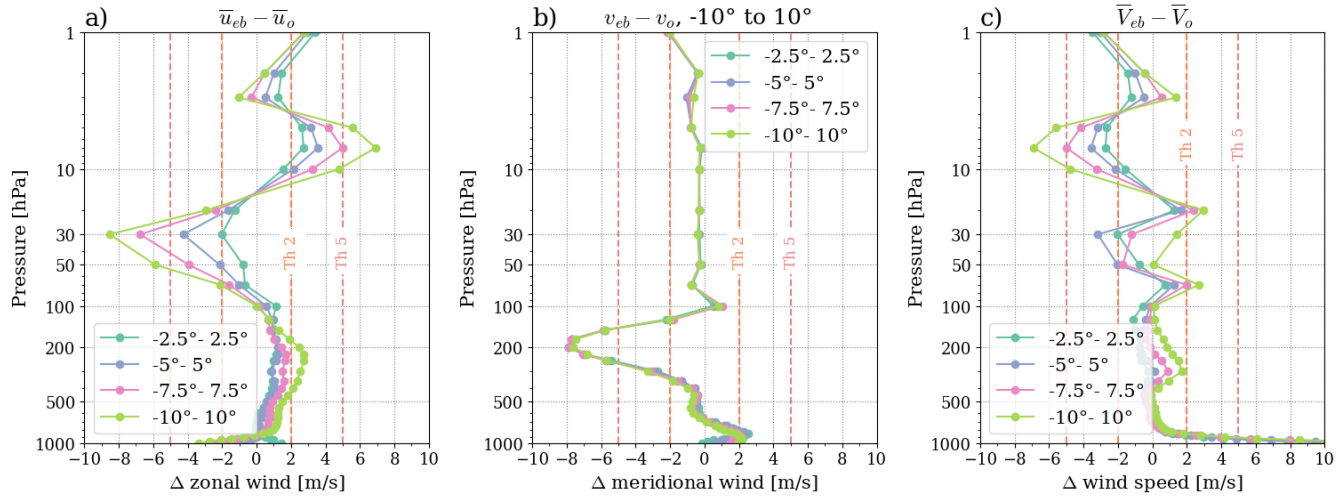

Figure 3. Equatorial balance bias of the calculated u, v and V components, calculated as a difference to the original components in ERA5. The deviation from the ERA5 data is shown for differently resolved latitude bands, to indicate the region around the equator where the approximation holds.

band is more pronounced, the latitudinal scope is therefore $-5°$ to $5°$. The meridional wind bias is very small below and above the tropopause.

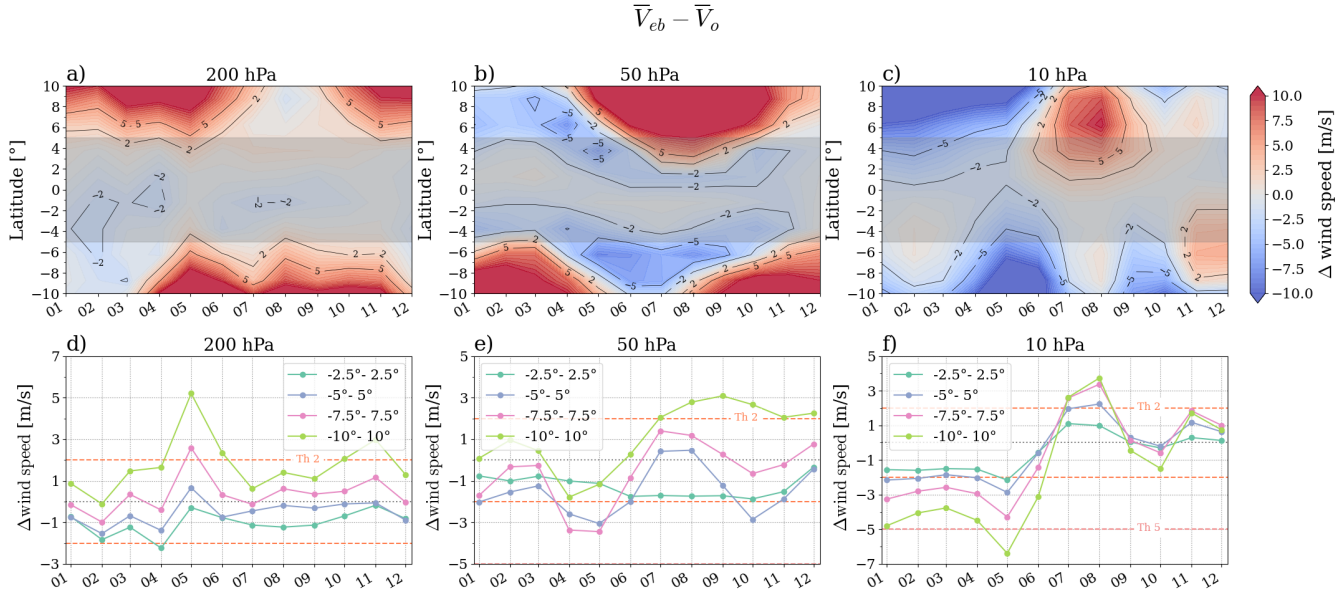

Figure 4. Temporal development of the bias resulting from the equatorial balance equation for the year 2009, based on ERA5 data.

https://doi.org/10.5194/amt-2023-137
Preprint. Discussion started: 13 July 2023

Atmospheric Measurement Techniques Discussions

In a final analysis in this section we investigate the bias resulting from the equatorial balance approximation for the complete year 2009 (Fig. 4). Our focus lies on the three representative levels, $200\,\mathrm{hPa}$, $50\,\mathrm{hPa}$ and $10\,\mathrm{hPa}$, relating roughly to the tropopause, lower stratosphere and middle stratosphere (Nimac et al., 2023). For all seasons the equatorial balance approximation is less accurate for lower pressures. For the lower stratosphere the region below the maximum bias threshold shifts away from the equator with the seasons, with an offset in the direction of the winter hemisphere. For $10\,\mathrm{hPa}$, the middle stratosphere, the approximation is least accurate during northern hemisphere summer months. When averaging from $-2.5°$ to $2.5°$ the wind speed bias stays below $\pm 2\,\mathrm{ms}^{-1}$ for nearly all months on all pressure levels. The bias increases for a broader latitudinal range.

4.2 RO wind validation

In this section we investigate the systematic data bias between RO and ERA5 reanalysis data. For RO u_{eb}, RO v_{eb} and RO V_{eb} the spatial patterns look very similar to the wind fields calculated with ERA5 data, see Fig. 5 top to bottom row, respectively. Between 30 hPa and 10 hPa the bias between the two data sets and for the zonal wind (u_{eb}, top row) lies between $\pm 2\,\mathrm{ms}^{-1}$ and $\pm 5\,\mathrm{ms}^{-1}$, increasing towards higher altitudes and exceeding the maximum threshold. A possible reason could be, that the impact of the residual ionospheric error, as well as measurement noise increase towards higher altitudes (e.g., Danzer et al., 2013, 2018; Liu et al., 2020). With the exception of this region and the boundary layer, the target threshold of $\pm 2\,\mathrm{ms}^{-1}$ is rarely exceeded.

Nimac et al. (2023) found that the bias between RO V_g and ERA V_g decreased after 2016, when ERA5 undertook a major observing system change. It is reasonable to assume that similar behavior could be observed for RO V_{eb} and ERA V_{eb}. We further note that with respect to RO data, the years 2008 and 2009 show a really high occultation statistics with a lot of available missions. In the years 2011 and 2012 there is a significant drop in the available occultations (Angerer et al., 2017). In those years we have no further data from the F3C-FM3 satellite, and also the SAC-C mission ended. However, with the launch of the COSMIC-2 mission in 2019, which is specifically designed for a high coverage in the tropics up to the mid-latitudes (Schreiner et al., 2020; Ho et al., 2020), the accuracy of RO data in the equatorial region will further increase. This possibly also allows to use a $-2.5°$x$2.5°$ wind field grid in future studies.

In a final analysis we investigate the development of the systematic data bias in wind speed for the complete year 2009 (see Fig. 6). There is little to no deviation of RO V_{eb} from ERA V_{eb} for the tropopause (200 hPa) and the lower stratosphere (50 hPa) all year. At the $10\,\mathrm{hPa}$ we observe somewhat larger deviations, most notable in the northern hemisphere summer months. The numbers of RO profiles accumulated to generate the monthly RO data set dropped by around 33% in June 2009 compared to other months in the same year. This decreases the data quality and therefore we observe an increase in the systematic data bias. The bias is within $\pm 2\,\mathrm{ms}^{-1}$ and $\pm 5\,\mathrm{ms}^{-1}$, indicating that towards high altitudes the wind speed retrieval over the tropics gets more challenging. We still see a potential for improvements in the ongoing work for correcting residual biases of RO data in the upper stratosphere (Danzer et al., 2021; Liu et al., 2020).

https://doi.org/10.5194/amt-2023-137
Preprint. Discussion started: 13 July 2023

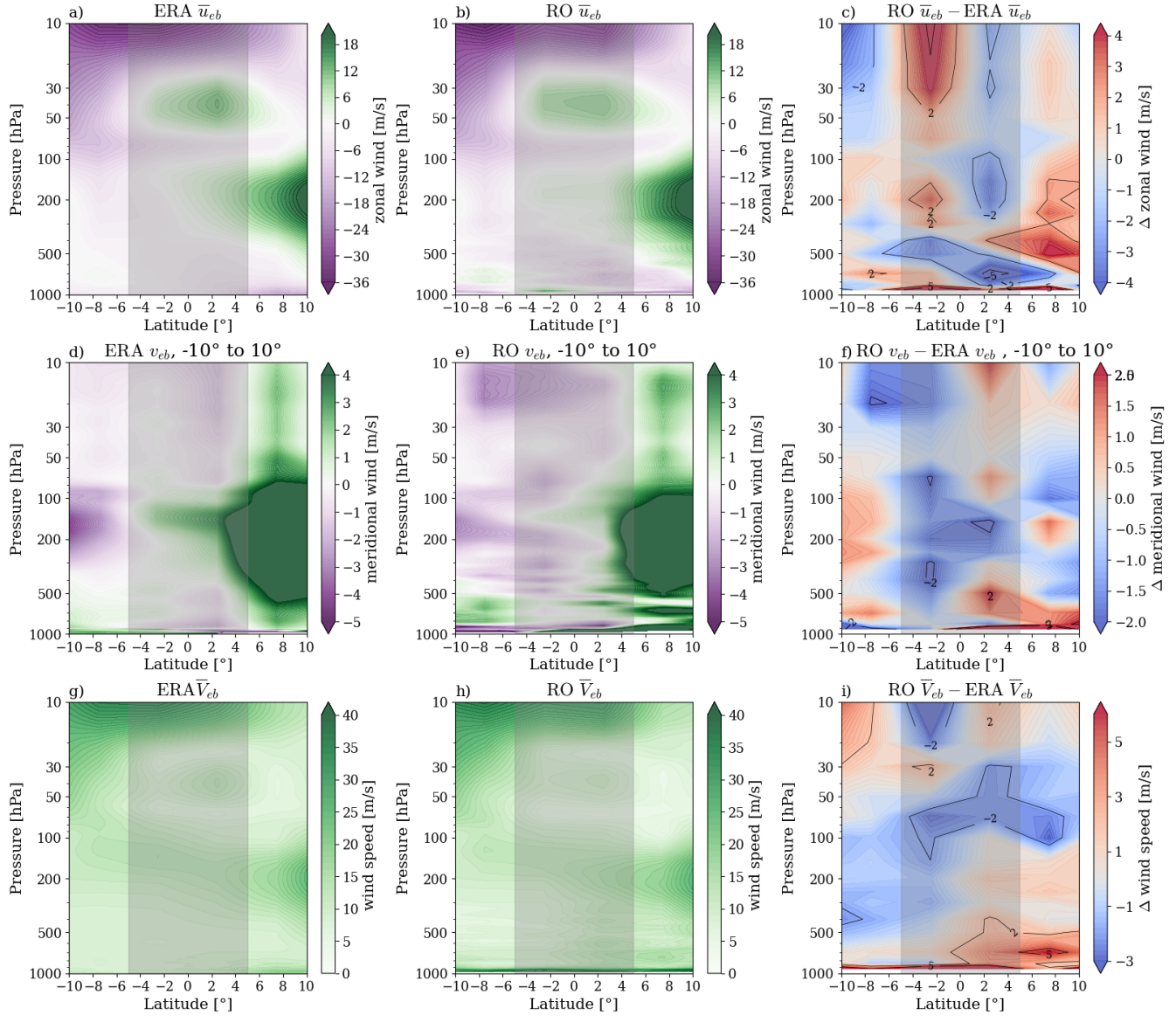

Figure 5. Panels a), d) and g) show the u, v and V components calculated with the equatorial balance approximation for ERA5 data, while panels b), e) and h) show the the same using RO data. The bottom row illustrates the difference between the values calculated between RO data and ERA5 data. Note that u and V are plotted as a zonal average, while the v component is shown as the mean of the longitude sector $-10°$ to $10°$.

https://doi.org/10.5194/amt-2023-137
Preprint. Discussion started: 13 July 2023

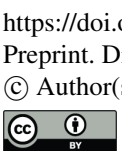

Atmospheric Measurement Techniques Discussions

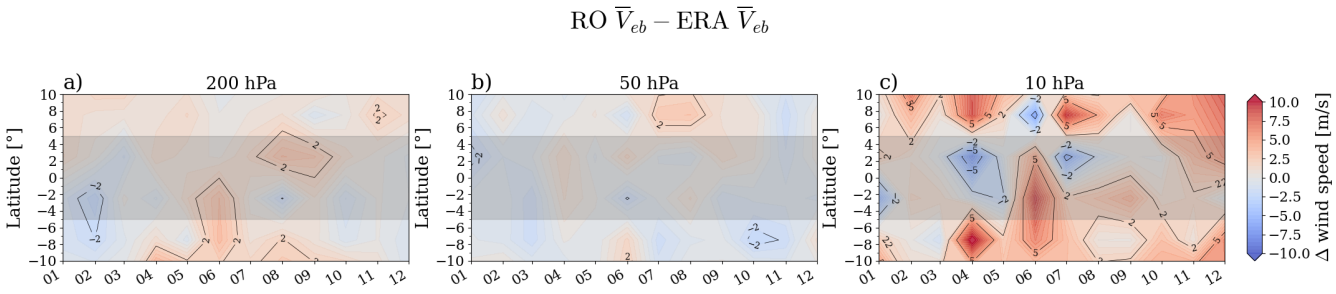

Figure 6. Temporal development of the systematic data bias between RO and ERA5 data, for the year 2009.

4.3 Closing the equatorial gap

In this final results sectionr, we aim to bridge the wind field gap over the equator, to complete with a wind field product over the complete globe. For this reason, we have once more a closer look at the zonal and meridional wind, as well as wind speed, at the three respective pressure levels 10 hPa, 50 hPa, and 200 hPa (first to third row, Fig. 7). In Fig. 7 we compare the computed winds, i.e., equatorial balance (eb) and geostrophic balance (g) RO and ERA5 winds, to original (o) ERA5 winds (black solid line). We analyze how the equatorial balance and geostrophic balance approximations bridge over the equator, thereby finding some interesting results. We observe that the zonal geostropic wind ($\overline{u}_g$) actually does not break down between $\pm 5°$, neither for RO or ERA5 computed winds. The results for $\overline{u}_g$ are actually closer to the original wind (black line, Fig. 7a, d, and g), than the computed zonal equatorial balanced winds (u_{eb}, RO and ERA5). The component that actually drives the geostrophic break down over the equator is the meridional wind component (v_g), showing the largest differences with respect to the original ERA5 meridional component (v_o) at 10 hPa, decreasing towards 200 hPa (Fig. 7b, e, and h). Here, the equatorial balance solution (v_{eb}, RO and ERA5) clearly better reproduces the ERA5 meridional winds, having the smallest bias at 200 hPa, with an increasing bias towards 10 hPa. Since the geostrophic meridional wind drives the equatorial breakdown (v_g), as a result, also the geostrophic wind speed (V_g) shows larger biases over the equator, while the equatorial wind speed (V_{eb}) is a better fit between $\pm 5°$ (Fig. 7c, f, and i).

Finally, we use our knowledge from the prior analysis to compute a complete global wind field data set, using RO data. In Fig. 8 we show the result based on the four seasonal representative months; January, April, July, and October. The wind fields are illustrated as a vertical cross section from 1000 hPa to 10 hPa, dependent on latitude. The l.h.s. of this plot (Fig. 8a, b, c, d) shows the bias between the computed RO wind fields, relative to ERA5 computed wind fields. Between $\pm 5°$ we use the equatorial balance equation for the calculation of the wind speed (V_{eb}), while outside this latitude band the geostrophic balance approximation is applied (V_g). We find that the bias between the two data sets is very low, with differences dominantly less than $\pm 2\,\mathrm{m\,s^{-1}}$. In the equatorial latitude band we find small exceedances in the lower troposphere, while the upper troposphere and lower stratosphere (UTLS) are very close to ERA5. This feature clearly relates to the core region of high quality RO data, which is in the UTLS. However, in the lower troposphere, the larger influence of moisture leads to a higher need of background information in the RO retrieval chain, and as a consequence to an increase in the bias in the RO data product.

https://doi.org/10.5194/amt-2023-137
Preprint. Discussion started: 13 July 2023

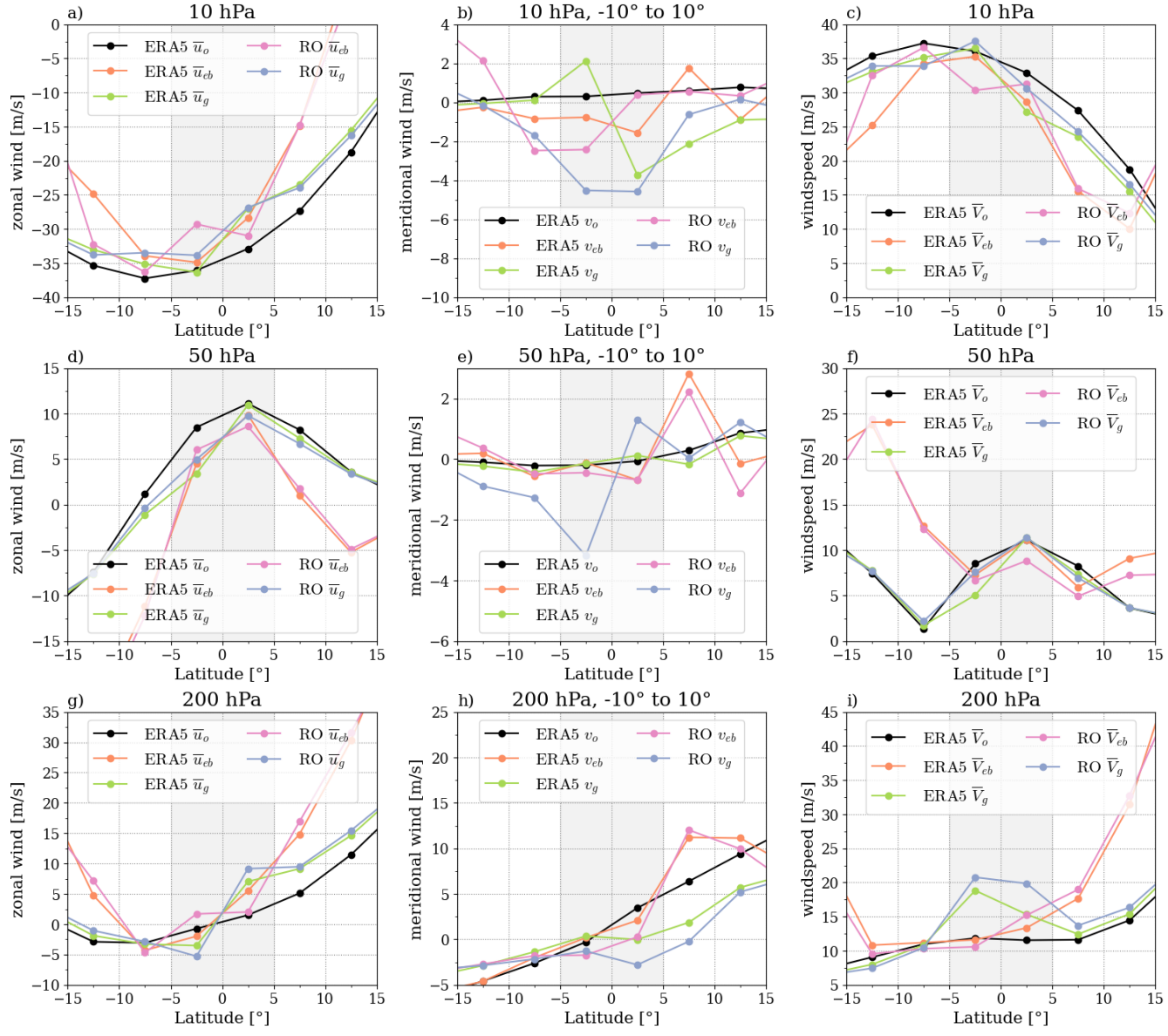

Figure 7. Detailed analysis of zonal wind (u, first column), meridional wind (v, second column), and wind speed (V, third column), at the three pressure levels 10 hPa, 50 hPa, and 200 hPa (first to third row). Results are shown for the original (o), equatorial-balanced (eb), geostrophic (g) ERA5 data and RO data (eb, g). u and V are plotted as the zonal mean, while the v component is calculated as a mean from the longitudinal sector -10° to 10°.

As a final comparison, we show on the r.h.s. of Fig. 8e, f, g, h, the respective RO wind fields relative to the original ERA5 wind data. We can conclude that the quality of the wind fields is especially above 500 hPa very good, and mostly within the required $\pm 2\,\mathrm{m\,s^{-1}}$. Outside this latitude band we apply the geostrophic approximation, and find also a high wind speed quality.

https://doi.org/10.5194/amt-2023-137
Preprint. Discussion started: 13 July 2023

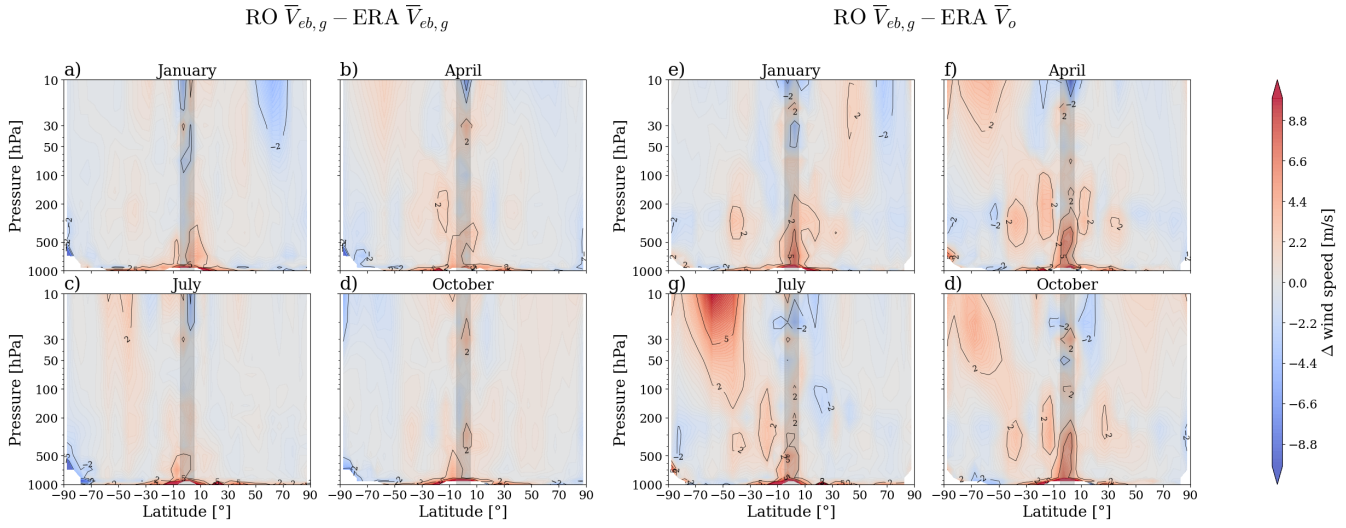

Figure 8. Zonal-mean wind speed bias, panels a) to d), and zonal-mean wind speed approximation bias, panels e) to h). To construct the RO and ERA wind fields, the equatorial balance equation is used inside the equatorial band (|Lat.| < 5, while outside this region the geostrophic balance approximation is used.

Exceptions are the stratospheric polar jet stream and the sub-tropical jet stream, where larger deviations are found. However, this was not part of this specific analysis. More information can be found in Nimac et al. (2023).

5 Summary and Conclusions

In this study we investigated the potential of radio occultation data for wind field monitoring in the tropics, with a specific focus on the equatorial area between $\pm 5°$ latitude. We analyzed the equatorial balance equation within this latitude band and computed wind fields on a 5° x 5° resolution. In a wider range over the tropics, we computed the RO wind fields using the geostrophic approximation, on a higher resolved 2.5° x 2.5° grid. We also calculated the winds using ERA5 data, applying the same physical equations and resolutions for the comparison analysis. In a first step, we analyzed the bias solely resulting from the equatorial balance approximation, by studying the difference between ERA5 computed winds and original winds. In a second step, we compared the RO computed winds to ERA5 computed winds. Finally, we analyzed how the geostrophic and equatorial balanced zonal winds, meridional winds, and wind speeds bridge towards the equator, to understand which wind component drives the geostrophic breakdown over the equator.

The results showed that we successfully could apply the equatorial balance equation for the RO wind field computation across the equator. A resolution of 5° x 5° was possible to obtain for the zonal and meridional wind components. However, especially the meridional wind component was a challenge, since the meridional wind speeds are in general much smaller than the zonal wind speeds, around $15\,\mathrm{ms}^{-1}$ compared to $1\,\mathrm{ms}^{-1}$, respectively. Hence, a wind flow with small magnitudes and also changes in the direction of the flow (changing sign) is challenging to reproduce. Nevertheless, the analysis clearly showed that

https://doi.org/10.5194/amt-2023-137
Preprint. Discussion started: 13 July 2023


Atmospheric Measurement Techniques Discussions

calculating both, the zonal and meridional wind components, resulted in a higher quality of the total wind speed fields (V). The biases were mostly within the target quality threshold of $\pm 2\,\mathrm{m\,s^{-1}}$, decreasing a bit in quality towards the 10 hPa level. At that point we emphasize that the COSMIC-2 mission (Schreiner et al., 2020; Ho et al., 2020), with a high occultation statistics in the tropics, will improve future RO wind fields in this area. Furthermore, the potential exists to go to even finer resolutions of 2.5° x 2.5° latitude x longitude.

A particularly interesting result was found when analyzing the individual wind components (u and v) and total wind speed (V), for geostrophic (g), equatorial balanced (eb), and original (o) winds, comparing RO and ERA5 data. We found that the dominant wind component, which drives the geostrophic breakdown, is the meridional wind, while the zonal geostrophic wind works very well also over the equator. The geostrophic zonal wind (u_g) performed even a bit better in quality than the equatorial zonal wind (u_{eb}). Nevertheless, the equatorial balance approximation works as a robust solution of the wind equation just over the latitude band $\pm 5°$. Outside this latitude band it is not the correct solution and hence breaks down. We tested also combinations of the total wind speed in this region, as a vector sum of zonal geostrophic wind and meridional equatorial wind in a specific altitude range. The results were quite satisfactory as well (not shown). To find a suitable combined wind construction is part of a future study.

To summarize, we find the results encouraging, since we see that RO data have the potential of long-term wind field monitoring over the complete globe, introducing across the equator.

Data availability. All computed wind field data for the year 2009 an be found under WEGC-cloud. The folder contains the following three files: (i) the wind field calculated from the WEGC Occultation Processing System OPSv5.6 RO data, (ii) the wind field calculated from ERA5 reanalysis data and further interpolated at the WEGC, and (iii) the wind field calculated from the download from the Copernicus Data store. The original RO OPSv5.6 data are available under WEGC-OPSv5.6

Author contributions. Conceptualization: JD, GK; Data curation: MP; Formal analysis: MP, JD; Funding acquisition: JD; Methodology: JD, GK; Supervision: JD, GK; Validation & Visualization: MP, JD, GK; Writing – original draft preparation: JD, MP; Writing – review & editing: JD, GK

Competing interests. The authors declare that they have no competing financial or personal interests.

Acknowledgements. We thank the UCAR/CDAAC RO team for providing RO excess phase and orbit data and the WEGC RO team for providing the OPSv5.6 retrieved profile data. We particularly thank F. Ladstädter (WEGC) for providing the monthly gridded climatology data. Furthermore, we thank the ECMWF for providing access to the ERA5 reanalysis data. We are also grateful for fruitful discussions with

https://doi.org/10.5194/amt-2023-137
Preprint. Discussion started: 13 July 2023

A. Osso. Finally, we thank the Austrian Science Fund (FWF) for funding the work; the wind analysis is part of the FWF stand-alone project Strato-Clim (grant number P-40182).

https://doi.org/10.5194/amt-2023-137
Preprint. Discussion started: 13 July 2023

References

Angerer, B., Ladstädter, F., Scherllin-Pirscher, B., Schwärz, M., Steiner, A. K., Foelsche, U., and Kirchengast, G.: Quality aspects of the Wegener Center multi-satellite GPS radio occultation record OPSv5. 6, Atmospheric Measurement Techniques, 10, 4845–4863, https://doi.org/10.5194/amt-2017-225, 2017.

Anthes, R.: Exploring Earth's atmosphere with radio occultation: contributions to weather, climate and space weather, Atmospheric Measurement Techniques, 4, 1077, 2011.

Anthes, R. A., Bernhardt, P. A., Chen, Y., Cucurull, L., Dymond, K. F., Ector, D., Healy, S. B., Ho, S.-P., Hunt, D. C., Kuo, Y.-H., Liu, H., Manning, K., McCormick, C., Meehan, T. K., Randel, W. J., Rocken, C., Schreiner, W. S., Sokolovskiy, S. V., Syndergaard, S., Thompson, D. C., Trenberth, K. E., Wee, T.-K., Yen, N. L., and Zeng, Z.: The COSMIC/FORMOSAT-3 mission: Early results, Bulletin of the American Meteorological Society, 89, 313–333, https://doi.org/10.1175/BAMS-89-3-313, 2008.

Bauer, P., Thorpe, A., and Brunet, G.: The quiet revolution of numerical weather prediction, Nature, 525, 47–55, 2015.

Beyerle, G., Schmidt, T., Michalak, G., Heise, S., Wickert, J., and Reigber, C.: GPS radio occultation with GRACE: Atmospheric profiling utilizing the zero difference technique, Geophysical Research Letters, 32, 2005.

Bodeker, G., Bojinski, S., Cimini, D., Dirksen, R., Haeffelin, M., Hannigan, J., Hurst, D., Leblanc, T., Madonna, F., Maturilli, M., et al.: Reference upper-air observations for climate: From concept to reality, Bulletin of the American Meteorological Society, 97, 123–135, 2016.

Cardinali, C. and Healy, S.: Impact of GPS radio occultation measurements in the ECMWF system using adjoint-based diagnostics, Quart. J. Roy. Meteor. Soc., 2014.

Chandra, S., Fleming, E. L., Schoeberl, M. R., and Barnett, J. J.: Monthly mean global climatology of temperature, wind, geopotential height and pressure for 0–120 km, Advances in Space Research, 10, 3–12, https://doi.org/10.1016/0273-1177(90)90230-W, 1990.

Cucurull, L.: Improvement in the use of an operational constellation of GPS radio occultation receivers in weather forecasting, Weather and Forecasting, 25, 749–767, 2010.

Danzer, J., Scherllin-Pirscher, B., and Foelsche, U.: Systematic residual ionospheric errors in radio occultation data and a potential way to minimize them, Atmospheric Measurement Techniques, 6, 2169–2179, https://doi.org/10.5194/amt-6-2169-2013, 2013.

Danzer, J., Schwärz, M., Proschek, V., Foelsche, U., and Gleisner, H.: Comparison study of COSMIC RO dry-air climatologies based on average profile inversion, Atmospheric Measurement Techniques, 11, 4867–4882, https://doi.org/10.5194/amt-11-4867-2018, 2018.

Danzer, J., Haas, S. J., Schwaerz, M., and Kirchengast, G.: Performance of the Ionospheric Kappa-Correction of Radio Occultation Profiles Under Diverse Ionization and Solar Activity Conditions, Earth and Space Science, 8, e2020EA001 581, 2021.

English, S., McNally, T., Bormann, N., Salonen, K., Matricardi, M., Moranyi, A., Rennie, M., Janisková, M., Di Michele, S., Geer, A., et al.: Impact of satellite data, 2013.

Eyre, J. R., English, S. J., and Forsythe, M.: Assimilation of satellite data in numerical weather prediction. Part I: The early years, Quarterly Journal of the Royal Meteorological Society, 146, 49–68, 2020.

Foelsche, U., Pirscher, B., Borsche, M., Kirchengast, G., and Wickert, J.: Assessing the climate monitoring utility of radio occultation data: From CHAMP to FORMOSAT-3/COSMIC, Terrestrial, Atmospheric and Oceanic Science, 20, 155–170, https://doi.org/10.3319/TAO.2008.01.14.01(F3C), 2009.

https://doi.org/10.5194/amt-2023-137
Preprint. Discussion started: 13 July 2023

Foelsche, U., Scherllin-Pirscher, B., Ladstädter, F., Steiner, A. K., and Kirchengast, G.: Refractivity and temperature climate records from multiple radio occultation satellites consistent within 0.05 %, Atmospheric Measurement Techniques, 4, 2007–2018, https://doi.org/10.5194/amt-4-2007-2011, 2011.

Hajj, G. A., Kursinski, E. R., Romans, L. J., Bertiger, W. I., and Leroy, S. S.: A technical description of atmospheric sounding by GPS occultation, Journal of Atmospheric and Solar-Terrestrial Physics, 64, 451–469, https://doi.org/10.1016/S1364-6826(01)00114-6, 2002.

Hajj, G. A., Ao, C., Iijima, B., Kuang, D., Kursinski, E., Mannucci, A., Meehan, T., Romans, L., de La Torre Juarez, M., and Yunck, T.: CHAMP and SAC-C atmospheric occultation results and intercomparisons, Journal of Geophysical Research: Atmospheres, 109, 2004.

Healy, S.: Operational assimilation of GPS radio occultation measurements at ECMWF, ECMWF Newsletter, 111, 6–11, 2007.

Healy, S. B., Polichtchouk, I., and Horányi, A.: Monthly and zonally averaged zonal wind information in the equatorial stratosphere provided by GNSS radio occultation, Quarterly Journal of the Royal Meteorological Society, 146, 3612–3621, https://doi.org/10.1002/qj.3870, 2020.

Hersbach, H., Bell, B., Berrisford, P., Hirahara, S., Horányi, A., Muñoz-Sabater, J., Nicolas, J., Peubey, C., Radu, R., Schepers, D., et al.: The ERA5 global reanalysis, Quarterly Journal of the Royal Meteorological Society, 146, 1999–2049, 2020.

Ho, S.-P., Zhou, X., Shao, X., Zhang, B., Adhikari, L., Kireev, S., He, Y., Yoe, J. G., Xia-Serafino, W., and Lynch, E.: Initial assessment of the COSMIC-2/FORMOSAT-7 neutral atmosphere data quality in NESDIS/STAR using in situ and satellite data, Remote Sensing, 12, 4099, 2020.

Holton, J. R.: An introduction to dynamic meteorology, no. v. 88 in International geophysics series, Elsevier Academic Press, Burlington, MA, 4th ed edn., oCLC: 54400282, 2004.

Kanitz, T., Lochard, J., Marshall, J., McGoldrick, P., Lecrenier, O., Bravetti, P., Reitebuch, O., Rennie, M., Wernham, D., and Elfving, A.: Aeolus first light: first glimpse, in: International Conference on Space Optics—ICSO 2018, vol. 11180, pp. 659–664, SPIE, 2019.

Kuo, Y.-H., Sokolovskiy, S. V., Anthes, R. A., and Vandenberghe, F.: Assimilation of GPS radio occultation data for numerical weather prediction, Terrestrial Atmospheric and Oceanic Sciences, 11, 157–186, 2000.

Kursinski, E. R., Hajj, G. A., Schofield, J. T., Linfield, R. P., and Hardy, K. R.: Observing Earth's atmosphere with radio occultation measurements using the Global Positioning System, Journal of Geophysical Research, 102, D19, https://doi.org/10.1029/97JD01569, 1997.

Ladstädter, F., Steiner, A., Schwärz, M., and Kirchengast, G.: Climate intercomparison of GPS radio occultation, RS90/92 radiosondes and GRUAN from 2002 to 2013, Atmospheric Measurement Techniques, 8, 1819–1834, 2015.

Ladstädter, F., Steiner, A. K., and Gleisner, H.: Resolving the 21st century temperature trends of the upper troposphere–lower stratosphere with satellite observations, Scientific Reports, 13, 1306, 2023.

Li, Y., Kirchengast, G., Schwaerz, M., and Yuan, Y.: Monitoring sudden stratospheric warmings under climate change since 1980 based on reanalysis data verified by radio occultation, Atmospheric Chemistry and Physics, 23, 1259–1284, 2023.

Liu, C., Kirchengast, G., Syndergaard, S., Schwaerz, M., and Danzer, J.: New higher-order correction of GNSS RO bending angles accounting for ionospheric asymmetry: evaluation of performance and added value, Remote Sensing, 12, 3637, https://doi.org/10.3390/rs12213637, 2020.

Luntama, J.-P., Kirchengast, G., Borsche, M., Foelsche, U., Steiner, A., Healy, S., von Engeln, A., O'Clerigh, E., and Marquardt, C.: Prospects of the EPS GRAS mission for operational atmospheric applications, Bulletin of the American Meteorological Society, 89, 1863–1876, 2008.

Nimac, I., Danzer, J., and Kirchengast, G.: Validation of the geostrophic approximation using ERA5 and the potential of long-term radio occultation data for supporting wind field monitoring, Atmospheric Measurement Techniques Discussions, 2023, 1–24, 2023.

https://doi.org/10.5194/amt-2023-137
Preprint. Discussion started: 13 July 2023

Scaife, A. A., Austin, J., Butchart, N., Pawson, S., Keil, M., Nash, J., and James, I. N.: Seasonal and interannual variability of the stratosphere diagnosed from UKMO TOVS analyses, Quarterly Journal of the Royal Meteorological Society, 126, 2585–2604, https://doi.org/10.1002/qj.49712656812, 2000.

Scherllin-Pirscher, B., Steiner, A. K., and Kirchengast, G.: Deriving dynamics from GPS radio occultation: Three-dimensional wind fields for monitoring the climate, Geophysical Research Letters, 41, 7367–7374, https://doi.org/10.1002/2014GL061524, 2014.

Scherllin-Pirscher, B., Steiner, A. K., Kirchengast, G., Schwärz, M., and Leroy, S. S.: The power of vertical geolocation of atmospheric profiles from GNSS radio occultation, Journal of Geophysical research: atmospheres, 122, 1595–1616, 2017.

Schreiner, W. S., Weiss, J., Anthes, R. A., Braun, J., Chu, V., Fong, J., Hunt, D., Kuo, Y.-H., Meehan, T., Serafino, W., et al.: COSMIC-2 radio occultation constellation: First results, Geophysical Research Letters, 47, e2019GL086 841, 2020.

Schwarz, J., Kirchengast, G., and Schwaerz, M.: Integrating uncertainty propagation in GNSS radio occultation retrieval: from bending angle to dry-air atmospheric profiles, Earth Space Sci., 4, 200–228, https://doi.org/10.1002/2016EA000234, 2017.

Schwarz, J., Kirchengast, G., and Schwaerz, M.: Integrating uncertainty propagation in GNSS radio occultation retrieval: from excess phase to atmospheric bending angle profiles, Atmospheric Measurement Techniques, 11, 2601–2631, https://doi.org/10.5194/amt-11-2601-2018, 2018.

Steiner, A., Lackner, B., Ladstädter, F., Scherllin-Pirscher, B., Foelsche, U., and Kirchengast, G.: GPS radio occultation for climate monitoring and change detection, Radio Science, 46, 1–17, https://doi.org/10.1029/2010RS004614, 2011.

Steiner, A. K., Ladstädter, F., Ao, C. O., Gleisner, H., Ho, S.-P., Hunt, D., Schmidt, T., Foelsche, U., Kirchengast, G., Kuo, Y.-H., et al.: Consistency and structural uncertainty of multi-mission GPS radio occultation records, Atmospheric Measurement Techniques, 13, 2547–2575, 2020.

Stoffelen, A., Pailleux, J., Källén, E., Vaughan, J. M., Isaksen, L., Flamant, P., Wergen, W., Andersson, E., Schyberg, H., Culoma, A., et al.: The atmospheric dynamics mission for global wind field measurement, Bulletin of the American Meteorological Society, 86, 73–88, 2005.

Stoffelen, A., Benedetti, A., Borde, R., Dabas, A., Flamant, P., Forsythe, M., Hardesty, M., Isaksen, L., Källén, E., Körnich, H., et al.: Wind profile satellite observation requirements and capabilities, Bulletin of the American Meteorological Society, 101, E2005–E2021, 2020.

Verkhoglyadova, O. P., Leroy, S. S., and Ao, C. O.: Estimation of winds from GPS radio occultations, Journal of Atmospheric and Oceanic Technology, 31, 2451–2461, 2014.

Wickert, J., Reigber, C., Beyerle, G., König, R., Marquardt, C., Schmidt, T., Grunwaldt, L., Galas, R., Meehan, T. K., Melbourne, W. G., et al.: Atmosphere sounding by GPS radio occultation: First results from CHAMP, Geophysical research letters, 28, 3263–3266, 2001.

Zeng, Z., Sokolovskiy, S., Schreiner, W. S., and Hunt, D.: Representation of Vertical Atmospheric Structures by Radio Occultation Observations in the Upper Troposphere and Lower Stratosphere: Comparison to High-Resolution Radiosonde Profiles, Journal of Atmospheric and Oceanic Technology, 36, 655–670, https://doi.org/10.1175/JTECH-D-18-0105.1, 2019.